J|A|C|S
ARTICLES
Published on Web 12/09/2006

Controlling the Helicity of 2,2′-Bipyridyl Ruthenium(II) and Zinc(II) Hemicage Complexes

Karl D. Oyler, Frederick J. Coughlin, and Stefan Bernhard*

Contribution from the Department of Chemistry, Princeton University, Princeton, New Jersey 08544

Received September 29, 2006; E-mail: bern@princeton.edu

Abstract: Two enantiomers of a new 4,5-pineno-2,2′-bipyridine ligand were synthesized and subsequently incorporated into hemicage ligands through a phenyl linker to yield ligands **(+)-L$_1$** and **(−)-L$_1$** or through a mesityl linker to yield ligands **(+)-L$_2$** and **(−)-L$_2$**. Complexation of these ligands to Ru(II) afforded diastereomerically pure Δ and Λ isomers, as verified through circular dichroism and circularly polarized luminescence spectroscopy. Ligands **(+)-L$_2$** and **(−)-L$_2$** were further coordinated to Zn(II) to form a complex with intriguing photophysical properties. Whereas $Zn(bpy)_3^{2+}$ was shown to be a fluorescent emitter outside the visible spectrum, the caging process provided an unprecedented enhancement of intersystem crossing and subsequent switching to the phosphorescent emission of blue light. Additionally, the chiroptical properties of the Zn(II) complexes were also studied.

Introduction

Enantiopure transition metal complexes have been and continue to be a subject of great interest because of their applicability toward such diverse areas as catalysis,[1] materials,[2] and chemical biology.[3] As a consequence of their typically charged nature, metal complex enantiomers and diastereomers are most commonly resolved through cocrystallization with chiral counterions, a fastidious methodology that was pioneered by Werner in 1911.[4] In contrast, direct stereoselective synthesis of metal complexes was largely unexplored throughout most of the 20th century. Over the past decade, however, much more attention has been paid to deliberate control of the helicity of metal complexes through synthetically tailored ligand systems.

Octahedral complexes of 2,2′-bipyridine (bpy) or 2-phenylpyridine (ppy) containing d^6 metals such as Ru(II), Os(II), and Ir(III) have been the focus of considerable research because of their established light-emitting and electron-transferring properties. As a result of the bidentate nature of these pyridyl ligands, the octahedral complexes formed from them will be one of two optical isomers, Δ or Λ; in the case of bidentate ligands of C_s symmetry such as phenylpyridine, facial (*fac*) and meridional (*mer*) isomers will also be present. For supramolecular assemblies possessing multiple metal centers coordinated to these types of ligands, such a variety of possible isomers can present a serious problem in that the characterization of these complexes through traditional means becomes difficult, if not impossible.[5]

In the past, complicated and time-consuming methods such as cocrystallization[6] or chiral solid-phase HPLC were required to separate the Δ and Λ isomers of metal complexes.[7−9] Further, even after being resolved, these species are susceptible to photoracemization, which may restore the racemic mixture over time and ruin the separation. To circumvent these problems, recent methods have centered on the use of caged ligand structures possessing chiral subsitituents.[10,11] Caged ligand structures present a number of advantages; in particular, their substitutional inertness makes them ideal for synthesizing metal complexes that are typically highly labile in solution, such as tris-diimine complexes of Fe(II) or Zn(II). Additionally, the rigid structure provided by caged ligands can greatly assist in reducing the rate constant for nonradiative decay (k_{nr}) and thus improve the quantum efficiency of luminescent metal complexes.[12,13]

Stereochemically, caged ligand systems are capable of predetermining *fac* or *mer* isomerism, but are not selective between the Δ and Λ isomers; for this to occur, further modification is necessary. In the recent past, this has been accomplished through the use of terpene-based substituents, most often pinene, as first implemented by Hayoz and von Zelewsky.[14] The chiral, steric bulk of such substituents can

(1) Inoue, Y.; Ramamurthy, V. *Chiral Photochemistry*; Marcel Dekker: New York, 2004; pp 261−313.
(2) Mamula, O.; von Zelewsky, A. *Coord. Chem. Rev.* **2003**, *242*, 87−95.
(3) Myari, A.; Hadjiliadis, N.; Garoufis, A. *J. Inorg. Biochem.* **2005**, *99*, 616−626.
(4) Werner, A. *Chem. Br.* **1911**, *44*, 1887−1890.
(5) von Zelewsky, A.; Mamula, O. *J. Chem. Soc., Dalton Trans.* **2000**, 219−231.
(6) Sagüés, J. A. A.; Gillard, R. D.; Smalley, D. H.; Williams, P. A. *Inorg. Chim. Acta* **1980**, *43*, 211−216.
(7) Rutherford, T. J.; Pellegrini, P. A.; Aldrich-Wright, J.; Junk, P. C.; Keene, F. R. *Eur. J. Inorg. Chem.* **1998**, 1677−1688.
(8) Fletcher, N. C.; Nieuwenhuyzen, M.; Rainey, S. *J. Chem. Soc., Dalton Trans.* **2001**, 2641−2648.
(9) Hesek, D.; Inoue, Y.; Everitt, S. R. L.; Ishida, H.; Kunieda, M.; Drew, M. G. B. *Inorg. Chem.* **2000**, *39*, 308−316.
(10) Hamann, C.; von Zelewsky, A.; Neels, A.; Stoeckli-Evans, H. *J. Chem. Soc., Dalton Trans.* **2004**, 402−406.
(11) Schaffner-Hamann, C.; von Zelewsky, A.; Barbieri, A.; Barigelletti, F.; Muller, G.; Riehl, J. P.; Neels, A. *J. Am. Chem. Soc.* **2004**, *126*, 9339−9348.
(12) Barigelletti, F.; De Cola, L.; Balzani, V.; Belser, P.; von Zelewsky, A.; Voegtle, F.; Ebmeyer, F.; Grammenudi, S. *J. Am. Chem. Soc.* **1989**, *111*, 4662−4668.
(13) Beeston, R. F.; Aldridge, W. S.; Treadway, J. A.; Fitzgerald, M. C.; DeGraff, B. A.; Stitzel, S. E. *Inorg. Chem.* **1998**, *37*, 4368−4379.
(14) Hayoz, P.; von Zelewsky, A. *Tetrahedron Lett.* **1992**, *33*, 5165−5168.

10.1021/ja067016v CCC: $37.00

directly lead to the preferential synthesis of a particular stereoisomer. Such caged metal complexes combine substitutional inertness with predetermined configuration at the metal center, thus making them ideal candidates for applications such as chromophores in stereogenic displays[15] or inducing chirality in other metal complexes through stereoselective photoinduced electron-transfer reactions.[16]

Here, we report on the synthesis of a new, pinene-substituted 2,2′-bipyridine ligand and its enantiomer with applicability toward fields such as asymmetric catalysis and the stereoselective formation of luminescent metal complexes. Through stereospecific alkylation of these ligands with phenyl or mesityl linking groups, we successfully synthesized hemicaged complexes of Ru(II) and blue-emitting Zn(II) with complete synthetic control of the helicity at the metal center as determined through circular dichroism (CD) and circularly polarized luminescence (CPL) spectroscopy.

Experimental Section

General. Reagents and solvents were purchased from Aldrich and used as received. The following were synthesized as described in the literature: 1-(2-acetylpyridyl)pyridinium bromide,[17] (1*R*,5*R*)-(+)-*β*-pinene,[18] 1,3,5-tris(bromomethyl)benzene,[19] (1*S*,5*R*)-(−)-nopinone and (1*R*,5*S*)-(+)-nopinone,[20] 5-methyl-2,2′-bipyridine,[21] $Ru(DMSO)_4Cl_2$,[22] $[Ru(bpy)_3]^{2+}(PF_6^-)_2$,[23] and $[Zn(bpy)_3]^{2+}(PF_6^-)_2$.[24] Varian/INOVA 400 and 500 MHz spectrometers were used to record ^{1}H NMR spectra; ^{13}C NMR data were obtained exclusively on the 500 MHz spectrometer (acquired at 125 MHz). A Hewlett-Packard 5898B (Electrospray) MS engine spectrometer was used to measure the mass spectra. Elemental analyses (CHN) were conducted by the Microanalytical Laboratory at the University of Illinois, Urbana-Champaign.

Δ-Hemicage Complexes. (1*R*,5*R*)-3-(Diethoxymethyl)nopinone (1). The synthesis was carried out according to the procedure described by Mock and Tsou.[25] Redistilled boron trifluoride diethyl etherate (13.5 mL, 0.110 mol) dissolved in 80 mL of dichloromethane was added dropwise over 20 min to triethyl orthoformate (14.9 mL, 0.090 mol) under nitrogen atmosphere at −30 °C. The mixture was then allowed to warm to 0 °C. After being stirred for 15 min, the mixture was cooled to −78 °C and 6.20 g (0.045 mol) of (1*R*,5*S*)-(+)-nopinone was added, followed by dropwise addition of *N*,*N*-diisopropylethylamine (23.5 mL, 0.135 mol). After being stirred for 1 h, the reaction mixture was poured into 600 mL of saturated aqueous sodium bicarbonate solution. An additional 250 mL of dichloromethane was then added, and the mixture was stirred for 10 min at room temperature. The organic layer was separated and washed with cold 1 M sulfuric acid followed by cold water. The organic phase was then dried with anhydrous sodium sulfate, and the solvent was removed by rotary evaporation to yield 8.66 g (80%) of orange, liquid product. ^{1}H NMR (500 MHz, $CDCl_3$): δ 0.76 (s, 3H), 1.01 (t, J = 7.02 Hz, 3H), 1.11 (t, J = 7.02 Hz, 3H), 1.20 (s, 3H), 1.78 (d, J = 10.07 Hz, 1H), 1.84 (t, J = 10.84 Hz, 1H), 2.08 (m, 2H), 2.29 (m, 1H), 2.37 (t, J = 5.34 Hz, 1H), 2.62 (m, 1H), 3.32 (m, 1H), 3.42 (m, 1H), 3.53 (m, 1H), 3.65 (m, 1H), 4.81 (d, J = 3.05 Hz, 1H). ^{13}C NMR (125 MHz, $CDCl_3$): δ 15.20, 15.42, 22.10, 22.20, 24.27, 26.10, 40.33, 40.77, 48.40, 58.17, 63.42, 65.08, 103.70, 212.81.

(1*R*,5*R*)-3-(Diethoxymethyl)nopinol (2). Under nitrogen atmosphere, **1** (8.00 g, 0.033 mol) was dissolved in 100 mL of anhydrous tetrahydrofuran and cooled to −78 °C. Lithium aluminum hydride (1.0 M in hexane, 40.0 mL, 0.043 mol) was added dropwise over 20 min. The mixture was then stirred for 1 h. The reaction was quenched through the slow addition of 20 mL of glacial acetic acid. The entire mixture was poured into 500 mL of hexanes, and an additional 400 mL of water was added. The layers were then separated, and the aqueous portion was extracted with hexanes (3 × 100 mL). The combined organic layers were dried with anhydrous sodium sulfate, and the solvent was removed by rotary evaporation to yield 7.40 g (94%) of **2**. ^{1}H NMR (400 MHz, $CDCl_3$): δ 0.63 (d, J = 10.07 Hz, 1H), 1.04 (s, 3H), 1.18 (m, 9H), 1.50 (m, 1H), 1.89 (s, 1H), 1.97 (m, 1H), 2.05 (m, 1H), 2.25 (m, 2H), 3.54 (m, 3H), 3.77 (m, 1H), 3.87 (m, 1H), 4.28 (d, J = 7.90 Hz, 1 H). The instability of **2** necessitated the next step to be carried out immediately, and ^{13}C NMR was not acquired.

(1*S*,5*R*)-Isomyrtenal (3). After **2** (7.40 g, 0.031 mol) was dissolved in 75 mL of tetrahydrofuran and 15 mL of 1 M hydrochloric acid, the solution was heated under reflux overnight. The reaction mixture was then poured into 150 mL of saturated aqueous sodium bicarbonate solution, followed by extraction (3 × 50 mL) with diethyl ether. The organic layer was dried with anhydrous sodium sulfate and rotary evaporated to yield 4.00 g (87%) of yellow, liquid product. ^{1}H NMR (500 MHz, $CDCl_3$): δ 0.75 (s, 3H), 1.30 (s, 3H), 2.21 (m, 1H), 2.45 (m, 3H), 7.32 (m, 1H), 9.42 (s, 1H). ^{13}C NMR (125 MHz, $CDCl_3$): δ 21.48, 26.25, 28.41, 31.47, 39.52, 39.79, 43.28, 139.11, 161.10, 193.28.

(7*R*,9*R*)-4,5-Pineno-2,2′-bipyridine (4). The ligand was prepared via a Kröhnke bipyridine synthesis.[26] Ammonium acetate (2.05 g, 0.027 mol), 1-(2-acetylpyridyl)pyridinium bromide (3.54 g, 0.013 mol), and **3** (1.91 g, 0.013 mol) were dissolved in 150 mL of methanol and heated under reflux overnight. The reaction mixture was poured into 150 mL of hexanes, and 150 mL of water was added. The layers were separated, and the aqueous portion was extracted with hexanes (4 × 50 mL). The combined organic layers were dried with anhydrous sodium sulfate, and the solvent was removed by rotary evaporation to yield 1.62 g (46%) of off-white crystals. ^{1}H NMR (500 MHz, $CDCl_3$): δ 0.70 (s, 3H), 1.28 (d, J = 9.46 Hz, 1H), 1.43 (s, 3H), 2.40 (m, 1H), 2.71 (m, 1H), 2.91 (t, J = 5.49 Hz, 1H), 3.05 (s, 2H), 7.30 (m, 1H), 7.81 (m, 1H), 8.01 (s, 1H), 8.38 (d, J = 7.94 Hz, 1H), 8.42 (s, 1H), 8.68 (m, 1H). ^{13}C NMR (125 MHz, $CDCl_3$): δ 21.58, 26.33, 30.51, 31.45, 39.16, 40.47, 47.72, 118.81, 121.24, 123.55, 131.42, 137.13, 148.28, 149.28, 153.69, 156.94, 157.19.

[(7*R*,9*R*,10*S*)-pbpyCH$_2$]$_3$Ph (pbpy = 4,5-Pineno-2,2′-bipyridine) ((−)-L$_1$). Under nitrogen atmosphere, **4** (1.00 g, 0.004 mol) was dissolved in 60 mL of anhydrous tetrahydrofuran and cooled to 0 °C. Lithium diisopropylamide (1.8 M in heptane/THF/ethylbenzene, 4.44 mL, 0.008 mol) was added dropwise over 15 min, and the resulting black solution was stirred for an additional 30 min. 1,3,5-Tris-(bromomethyl)benzene (0.280 g, 7.84 × 10^{-4} mol) was added in small portions over 1 h, and the solution was stirred overnight. The reaction mixture was then poured into 200 mL of 10% ammonium chloride solution. The layers were separated, and the aqueous portion was extracted (3 × 75 mL) with diethyl ether. The combined organic fractions were dried with anhydrous sodium sulfate, and the solvent was removed by rotary evaporation to give an orange oil. The product was purified by column chromatography on silica gel using a 3:2 ethyl acetate/hexanes eluent to give 0.170 g (24%) of solid, yellow product. ^{1}H NMR (500 MHz, $CDCl_3$): δ 0.63 (s, 3H), 1.39 (s, 3H), 1.47 (d, J = 9.77 Hz, 1H), 2.07 (s, 1H), 2.58 (m, 1H), 2.81 (t, J = 11.60 Hz,

(15) Chen, S. H.; Katsis, D.; Schmid, A. W.; Mastrangelo, J. C.; Tsutsui, T.; Blanton, T. N. *Nature* **1999**, *397*, 506−508.
(16) Hamada, T.; Ohtsuka, H.; Sakaki, S. *J. Chem. Soc., Dalton Trans.* **2001**, 928−934.
(17) Mürner, H.; von Zelewsky, A.; Stoeckli-Evans, H. *Inorg. Chem.* **1996**, *35*, 3931−3935.
(18) Brown, H. C.; Zaidlewicz, M.; Bhat, K. S. *J. Org. Chem.* **1989**, *54*, 1764−1766.
(19) Ilioudis, C. A.; Tocher, D. A.; Steed, J. W. *J. Am. Chem. Soc.* **2004**, *126*, 12395−12402.
(20) Brown, H. C.; Weissman, S. A.; Perumal, P. T.; Dhokte, U. P. *J. Org. Chem.* **1990**, *55*, 1217−1223.
(21) Polin, J.; Schmohel, E.; Balzani, V. *Synthesis* **1998**, 321−324.
(22) Evans, I. P.; Spencer, A.; Wilkinson, G. *J. Chem. Soc., Dalton Trans.* **1973**, 204−209.
(23) Bernhard, S.; Barron, J. A.; Houston, P. L.; Abruña, H. D.; Ruglovksy, J. L.; Gao, X.; Malliaras, G. G. *J. Am. Chem. Soc.* **2002**, *124*, 13624−13628.
(24) Chlistunoff, J. B.; Bard, A. J. *Inorg. Chem.* **1993**, *32*, 3521−3527.
(25) Mock, W. L.; Tsou, H. R. *J. Org. Chem.* **1981**, *46*, 2557−2561.
(26) Kröhnke, F. *Synthesis* **1976**, 1−24.

1H), 2.93 (t, J = 5.04 Hz, 1H), 3.39 (m, 2H), 7.01 (s, 1H), 7.30 (m, 1H), 7.83 (t, J = 7.78 Hz, 1H), 8.04 (s, 1H), 8.40 (d, J = 7.93 Hz, 1H), 8.62 (s, 1H), 8.69 (d, J = 3.97 Hz, 1H). ^{13}C NMR (125 MHz, $CDCl_3$): δ 21.18, 26.61, 27.63, 40.22, 41.13, 41.15, 43.62, 48.26, 118.66, 121.33, 123.67, 128.23, 134.86, 137.16, 140.60, 148.00, 149.33, 154.04, 156.80, 156.96. $[\alpha]_D$ −34° (25 °C, 5 mg in 5 mL of $CHCl_3$).

[(7*R*,9*R*,10*S*)-pbpyCH$_2$]$_3$Ph(CH$_3$)$_3$ ((−)-L$_2$). The ligand was prepared via the procedure identical to that for **(−)-L$_1$**, substituting 0.638 g (1.60 mmol) of tris(bromomethyl)mesitylene for 1,3,5-tris(bromomethyl)benzene and reacting with **4** (2.00 g, 8.00 mmol) and lithium diisopropylamide (1.8 M in heptane/THF/ethylbenzene, 4.00 mL, 8.00 mmol) to yield 0.516 g (36%) after purification. ^{1}H NMR (500 MHz, $CDCl_3$): δ 0.61 (s, 9H), 1.35 (s, 9H), 1.59 (d, J = 9.77 Hz, 3H), 2.03 (m, 3H), 2.44 (s, 9H), 2.66 (m, 3H), 2.93 (t, J = 5.34 Hz, 9H), 3.15 (m, 3H), 3.30 (d, J = 10.99 Hz, 3H), 3.39 (dd, J_1 = 4.12 Hz, J_2 = 14.19), 7.31 (m, 3H), 7.82 (t, J = 7.63 Hz, 3H), 8.06 (s, 3H), 8.41 (d, J = 7.63 Hz, 3H), 8.65 (s, 3H), 8.68 (m, 3H). ^{13}C NMR (125 MHz, $CDCl_3$): δ 21.01, 26.61, 29.03, 34.76, 41.08, 41.14, 43.82, 48.27, 118.69, 121.40, 123.74, 134.18, 135.08, 135.85, 137.21, 147.65, 147.78, 149.32, 156.45, 156.66. $[\alpha]_D$ −183° (25 °C, 5 mg in 5 mL $CHCl_3$).

Δ-[Ru((−)-L$_1$)](PF$_6$)$_2$ (7). **(−)-L$_1$** (0.100 g, 0.116 mmol) was dissolved in 100 mL of hot ethanol, and $Ru(DMSO)_4Cl_2$ (0.056 g, 0.116 mmol) was added in small portions over 30 min. The red solution was heated under reflux for 3 h before removal of the solvent by rotary evaporation. The resulting red solid was then dissolved in 50 mL of water, and a solution of ammonium hexafluorophosphate (1.00 g) in 5 mL of water was added to precipitate the ruthenium complex as a PF_6^- salt. The complex was separated by filtration, dissolved in acetone, and filtered through a short column of aluminum oxide to remove polymeric impurities. Following evaporation of the solvent from the filtrate, recrystallization by vapor diffusion of acetonitrile and ether yielded 0.030 g (21%) of pure product. ^{1}H NMR (500 MHz, d_6-acetone): δ 0.36 (s, 9H), 1.48 (s, 9H), 1.86 (d, J = 10.38 Hz, 3H), 2.40 (m, 3H), 2.87 (m, 6H), 3.12 (t, J = 5.49 Hz, 3H), 3.29 (m, 3H), 3.67 (m, 3H), 7.36 (s, 3H), 7.41 (d, J = 5.19 Hz, 3H), 7.47 (m, 1H), 7.76 (s, 3H), 8.13 (t, J = 7.64 Hz, 3H), 8.40 (s, 3H), 8.69 (d, J = 8.24 Hz, 3H). ^{13}C NMR (125 MHz, d_6-acetone): δ 20.30, 25.55, 28.22, 39.23, 41.47, 41.85, 47.01, 48.50, 121.05, 124.16, 127.31, 130.91, 137.62, 138.06, 140.63, 150.09, 151.00, 154.51, 157.87, 158.34. MS (m/z; ESI): 1111 (1%, $M^{2+} - PF_6^-$), 483 (100%, $M^{2+} - 2PF_6^-$). Anal. Calcd for $C_{60}H_{60}N_6Ru(PF_6)_2 \cdot 2H_2O$: C, 55.77; H, 4.99; N, 6.50. Found: C, 55.97; H, 5.00; N, 6.13.

Δ-[Ru((−)-L$_2$)](PF$_6$)$_2$ (8). The procedure identical to that for **7** was used, substituting 0.100 g (0.110 mmol) of ligand **(−)-L$_2$** in place of **(−)-L$_1$**. Complexation with $Ru(DMSO)_4Cl_2$ (0.053 g, 0.110 mmol) and recrystallization yielded 0.039 g (27%). ^{1}H NMR (500 MHz, d_6-acetone): δ 0.34 (s, 9H), 1.49 (s, 9H), 2.02 (d, J = 10.38 Hz, 3H), 2.23 (s, 9H), 2.45 (m, 3H), 2.97 (m, 3H), 3.15 (m, 9H), 3.62 (t, J = 8.24 Hz, 3H), 7.35 (s, 3H), 7.47 (m, 3H), 7.50 (d, J = 4.58 Hz, 3H), 8.13 (t, J = 7.63 Hz, 3H), 8.40 (s, 3H), 8.67 (d, J = 8.24 Hz, 3H). ^{13}C NMR (125 MHz, d_6-acetone): δ 17.66, 20.29, 25.60, 28.08, 35.81, 37.53, 42.46, 46.93, 48.45, 121.17, 124.13, 127.35, 135.05, 136.60, 137.51, 137.61, 149.66, 151.10, 151.10, 154.56, 158.04, 158.13. MS (m/z; ESI): 1155 (4%, $M^{2+} - PF_6^-$), 504 (100%, $M^{2+} - 2PF_6^-$). Anal. Calcd for $C_{63}H_{66}N_6Ru(PF_6)_2 \cdot 2H_2O$: C, 56.71; H, 5.29; N, 6.30. Found: C, 56.69; H, 5.27; N, 6.09.

Δ-[Zn((−)-L$_2$)](PF$_6$)$_2$ (9). The complex was prepared by dissolving **(−)-L$_2$** (0.050 g, 0.058 mmol) in hot ethanol (100 mL) along with $ZnCl_2$ (0.008 g, 0.058 mmol) and refluxing for 4 h. The solvent was removed by rotary evaporation, and the resulting white solid was dissolved in 50 mL of water and then treated with 1.00 g of NH_4PF_6 (dissolved in 5 mL of water) to precipitate the complex. Subsequent filtering and recrystallization via vapor diffusion of acetonitrile/ether gave 0.040 g (57%) of pure metal complex. ^{1}H NMR (500 MHz, d_6-acetone): δ 0.34 (s, 9H), 1.47 (s, 9H), 1.91 (d, J = 10.38 Hz, 3H), 2.25 (s, 9H), 2.44 (m, 3H), 2.94 (m, 3H), 3.16 (m, 9H), 3.62 (t, J = 8.25 Hz, 3H), 7.53 (s, 3H), 7.61 (m, 3H), 7.72 (d, J = 4.27 Hz, 3H), 8.30 (t, J = 7.63 Hz, 3H), 8.38 (s, 3H), 8.66 (d, J = 8.24 Hz, 3H). ^{13}C NMR (125 MHz, d_6-acetone): δ 17.54, 20.34, 25.59, 28.00, 35.75, 37.55, 42.16, 46.98, 48.78, 120.49, 123.32, 127.53, 135.18, 136.63, 136.88, 141.93, 146.93, 147.02, 147.94, 150.05, 162.37. MS (m/z; ESI): 1117 (2%, $M^{2+} - PF_6^-$), 485 (100%, $M^{2+} - 2PF_6^-$). Anal. Calcd for $C_{63}H_{66}N_6Zn(PF_6)_2 \cdot 2H_2O$: C, 58.27; H, 5.43; N, 6.47. Found: C, 58.48; H, 5.17; N, 6.39.

Λ-Hemicage Complexes. The **(+)-L$_1$** and **(+)-L$_2$** ligands were synthesized starting from (1*S*,5*R*)-(−)-nopinone and otherwise prepared in a fashion similar to the procedures described above. Λ-Ru(II) complexes were prepared from both **(+)-L$_1$** and **(+)-L$_2$**, while a Λ-Zn(II) complex was prepared from **(+)-L$_2$**.

Racemic Hemicages. [bpy(CH$_2$)$_2$]$_3$Ph(CH$_3$)$_3$ (L$_3$). 5-Methyl-2,2′-bipyridine (4.14 g, 0.0245 mol) was dissolved with stirring in 100 mL of anhydrous THF at −78 °C under N_2. Lithium diisopropylamide (2.0 M in heptane/THF/ethylbenzene, 12.25 mL, 0.0245 mol) was added dropwise by syringe over 30 min; the resulting black solution was then stirred for an additional 15 min. Tris(bromomethyl)mesitylene (1.95 g, 0.00490 mol) was dissolved in 50 mL of anhydrous THF and added dropwise by syringe over 3 h. After being stirred for an additional hour, the black solution was poured into 500 mL of hexanes, forming a cloudy blue mixture that gradually turned yellow. After being filtered, the yellow solid was washed with hexanes and then dissolved in 500 mL of CH_2Cl_2. The solution was washed with 10% NH_4Cl solution and backwashed with water, and then the combined organic layers were dried over Na_2SO_4 (s) and concentrated to dryness by rotary evaporation to yield 2.90 g (89%) of yellow, solid product of sufficient purity to carry out metal complexation reactions. For characterization experiments, the ligand was further purified by recrystallization from hexanes/dichloromethane. ^{1}H NMR (400 MHz, $CDCl_3$): δ 2.37 (s, 9H), 2.84 (m, 6H), 3.05 (m, 6H), 7.30 (m, 3H), 7.68 (dd, J_1 = 8.13 Hz, J_2 = 2.24 Hz, 3H), 7.82 (td, J_1 = 7.55 Hz, J_2 = 1.81 Hz, 3H), 8.37 (m, 6H), 8.56 (s, 3H), 8.69 (m, 3H). ^{13}C NMR (125 MHz, $CDCl_3$): δ 16.25, 32.73, 33.00, 121.15, 123.82, 132.59, 136.39, 137.10, 137.27, 137.81, 149.33, 149.37, 154.29, 156.26.

Δ/Λ-[Ru(L$_3$)](PF$_6$)$_2$ (11). The complex was prepared via a procedure identical to that for **7**. **L$_3$** (0.100 g, 0.149 mmol) and $Ru(DMSO)_4Cl_2$ (0.072 g, 0.149 mmol) were combined to give 0.035 g (22%) of product. ^{1}H NMR (500 MHz, d_6-acetone): δ 1.96 (s, 9H), 2.77 (m, 3H), 2.92 (m, 3H), 3.07 (m, 3H), 3.31 (m, 3H), 6.49 (d, J = 1.46 Hz, 3H), 7.51 (td, J_1 = 6.23 Hz, J_2 = 1.46 Hz, 3H), 8.06 (d, J = 5.49 Hz, 3H), 8.12 (td, J_1 = 7.69 Hz, J_2 = 1.46 Hz, 3H), 8.28 (dd, J_1 = 8.42 Hz, J_2 = 1.83 Hz, 3H), 8.65 (t, J = 8.06 Hz, 6H). ^{13}C NMR (125 MHz, d_6-acetone): δ 16.92, 29.50, 30.89, 124.29, 127.74, 134.06, 134.85, 138.01, 138.55, 141.08, 151.74, 151.88, 154.96, 157.30. MS (m/z; ESI): 913 (5%, $M^{2+} - PF_6^-$), 384 (100%, $M^{2+} - 2PF_6^-$). Anal. Calcd for $C_{45}H_{42}N_6Ru(PF_6)_2 \cdot 2H_2O$: C, 49.41; H, 4.24; N, 7.68. Found: C, 49.68; H, 4.16; N, 7.68.

Δ/Λ-[Zn(L$_3$)](PF$_6$)$_2$ (12). The complex was prepared by dissolving **L$_3$** (0.100 g, 0.150 mmol) in hot ethanol (200 mL) followed by the addition of NH_4PF_6 (0.200 g) and $ZnCl_2$ (0.020 g, 0.130 mmol). After being refluxed overnight, 100 mL of solution was removed by rotary evaporation, leading to the precipitation of white product. Subsequent filtering and recrystallization via vapor diffusion of acetonitrile/ether gave 0.090 g (58%) of the pure metal complex. ^{1}H NMR (400 MHz, d_6-acetone): δ 2.08 (s, 9H), 2.90 (m, 3H), 3.00 (m, 3H), 3.15 (m, 3H), 3.38 (m, 3H), 6.63 (s, 3H), 7.73 (t, J = 1.10 Hz, 3H), 8.37 (t, J = 7.87 Hz, 3H), 8.41 (d, J = 4.76 Hz, 3H), 8.52 (d, 8.06 Hz, 3H), 8.76 (d, J = 8.05 Hz, 6H). ^{13}C NMR (125 MHz, d_6-acetone): δ 16.90, 29.50, 30.82, 123.26, 123.58, 127.59, 134.08, 134.89, 141.00, 142.06, 142.61, 147.06, 148.39, 148.64, 149.57. MS (m/z; ESI): 876 (17%, $M^{2+} - PF_6^-$), 365 (100%, $M^{2+} - 2PF_6^-$). Anal. Calcd for $C_{45}H_{42}N_6Zn(PF_6)_2 \cdot 1.5H_2O$: C, 51.51; H, 4.32; N, 8.01. Found: C, 51.42; H, 3.96; N, 7.82.

Photophysical Measurements. All photophysical measurements were carried out in acetonitrile solution. UV−visible spectra were recorded at room temperature in a 1.0-cm quartz cuvette using a Hewlett-Packard 8453 spectrometer. CD spectra were collected by an AVIV-62DS circular dichroism spectrometer and measured at room temperature in a 1.0-cm quartz cuvette. Data points were collected at 1-nm intervals using averaging times of 1 s/nm with a spectral bandwidth of 1.5 nm and sample concentrations of 25 μM. Optical rotation data were obtained by a PE model 341 polarimeter with a tube length of 1 dm.

Emission spectra were recorded using a Jobin-Yvon Fluorolog-3 spectrometer equipped with a double monochromator and a Hamamatsu-928 photomultiplier tube (PMT) as the detector. Excitation occurred at 450 nm for the Ru(II) compounds and at 315 nm for the Zn(II) complexes.

Excited-state lifetimes were measured by exciting the samples at 337 nm with an N_2 laser (Laser Science, Inc., VSL-337LRF, 10-ns pulse) or by the fourth harmonic (266 nm) of a Nd:YAG (Continuum Minilite) laser. The apparatus was connected to the Jobin-Yvon Fluorolog-3 spectrometer, utilizing the emission monochromator and PMT detector. The detector was in turn connected to a Tektronix TDS 3032B digital phosphor oscilloscope.

Circularly Polarized Luminescence Spectroscopy. The emission of the samples was detected at a 90° angle to the excitation in a Jobin-Yvon Fluorolog-3 and was passed through a photoelastic modulator (Hinds International PEM-90, operating at a modulation frequency of 50 kHz), followed by a linear polarizer. The light was then incident upon the emission monochromator. A Hamamatsu-928 PMT in conjunction with a gated photon counter (Stanford Research SR 400) was used to acquire the CPL spectrum.[27]

CPL measurements of the Ru(II) compounds were made over several 15-h periods. The photon counter gates were open for 30% (6 μs) of the duty cycle of the PEM; two gates were used, each centered around the extrema of the sinusoidal modulation cycle. The excitation light for the Ru(II) complexes was 450 nm, with a slit width of 10 nm, and the emission monochromator had a slit width of 6 nm.

The CPL measurements for the Zn(II) compounds were taken over a 2.5 h period. The excitation was at 315 nm with a slit width of 5 nm, and the emission monochromator had a slit width of 5 nm.

Owing to the difficulty in calculating absolute emission intensities, the ratio of the differential emission intensity (ΔI) to the total intensity (I) is reported as the emission dissymmetry ratio (g_{em}) in eq 1:

$$g_{em}(\lambda) = \frac{\Delta I}{{}^1/_2 I} = \frac{I_L - I_R}{{}^1/_2(I_L + I_R)} \quad (1)$$

Here, I_L and I_R refer to the left and right circularly polarized luminescence, respectively.

To ensure that there was no bias toward one type of circularly polarized light, a solution containing racemic $[Ru(\mathbf{L_3})](PF_6)_2$ was measured. A slight bias was found, as the average value of g_{em} was -7.9×10^{-5}. To adjust for this, ΔI for all CPL measurements was corrected using eq 2.

$$\Delta I_{corr} = \Delta I_{exp} + \frac{7.9 \times 10^{-5}}{2} I_{exp} \quad (2)$$

Results and Discussion

Synthesis. The chiral pinene ring can be fused to the 2,2′-bipyridine ligand in either the 4,5 (Figure 1a,c) or the 5,6 position (Figure 1b). Because of strong steric crowding near the nitrogen donor atom on the pyridine ring, 5,6-substituted 2,2′-bipyridines do not bond well to octahedral-coordinating metals,[2] so our synthetic strategy was focused on modifying the 4,5-pineno-2,2′-bipyridine. Apart from the chiral nature of the substituents, one of the key features of the pineno-2,2′-bipyridines is the customizability provided by the acidic $-CH_2-$ group found on the pinene ring (highlighted in red in Figure 1). This group can be easily deprotonated with a base such as LDA and stereospecifically substituted with a variety of electrophiles.

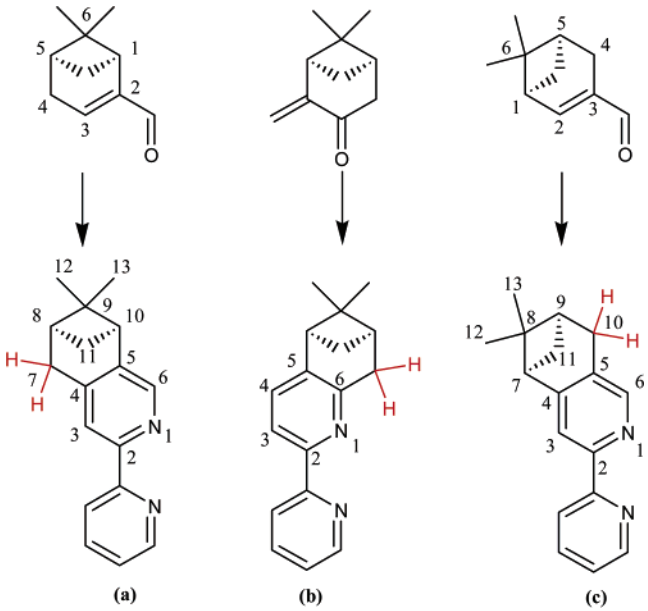

Figure 1. (a) 4,5-Pinene bipyridyl ligand synthesized from myrtenal by von Zelewsky and co-workers. (b) 5,6-Pinene bipyridyl ligand synthesized from pinocarvone. (c) 4,5-Pinene bipyridyl ligand reported in this article and synthesized from iso-myrtenal. The acidic protons in each molecule are highlighted in red.

In previous work involving the 4,5-substituted complexes, myrtenal was used as a precursor for the Kröhnke step, which finalizes the bipyridine synthesis.[14] The ligand can be deprotonated and substituted at the 7 position (Figure 1a), a location that leads to two major drawbacks: (1) because the reactive site faces the opposite direction to the chelating diimine moiety, adding substituents to the ligand is unlikely to cause any improvement to enantioselective catalytic processes, and (2) geometric constraints make it extremely difficult to form a caged metal complex using a simple linker between the three bipyridyl subunits; to successfully form the complex, long chain spacer groups containing ether linkages have been required.[10]

To address these issues, we endeavored to synthesize a modified 4,5-pineno-2,2′-bipyridine ligand with the acidic $-CH_2-$ protons located in a more advantageous location. Our synthetic pathway resulted in the rotation of the pinene moiety, thus moving the acidic methylene group to position 10 (Figure 1c, bottom). Following deprotonation and substitution with a suitable cap, a hemicage ligand that was capable of coordinating to a divalent transition metal ion was successfully prepared. This approach necessitated the synthesis of a myrtenal isomer precursor, which possesses a carboxaldehyde group at position 3 (Figure 1c, top) as compared to the myrtenal case where the carboxaldehyde is attached at position 2 (Figure 1a, top).

Figure 2 outlines the synthesis of the chiral, pinenobipyridyl hemicage ligands. The process consists of six synthetic steps and is highlighted by a Kröhnke bipyridine synthesis.[26] Ligands **(+)-L₂** and **(−)-L₂** differ from the **L₁** ligands by the presence

(27) Schippers, P. H.; van den Beukel, A.; Dekkers, H. P. J. M. *J. Phys. E* **1982**, *15*, 945−950.

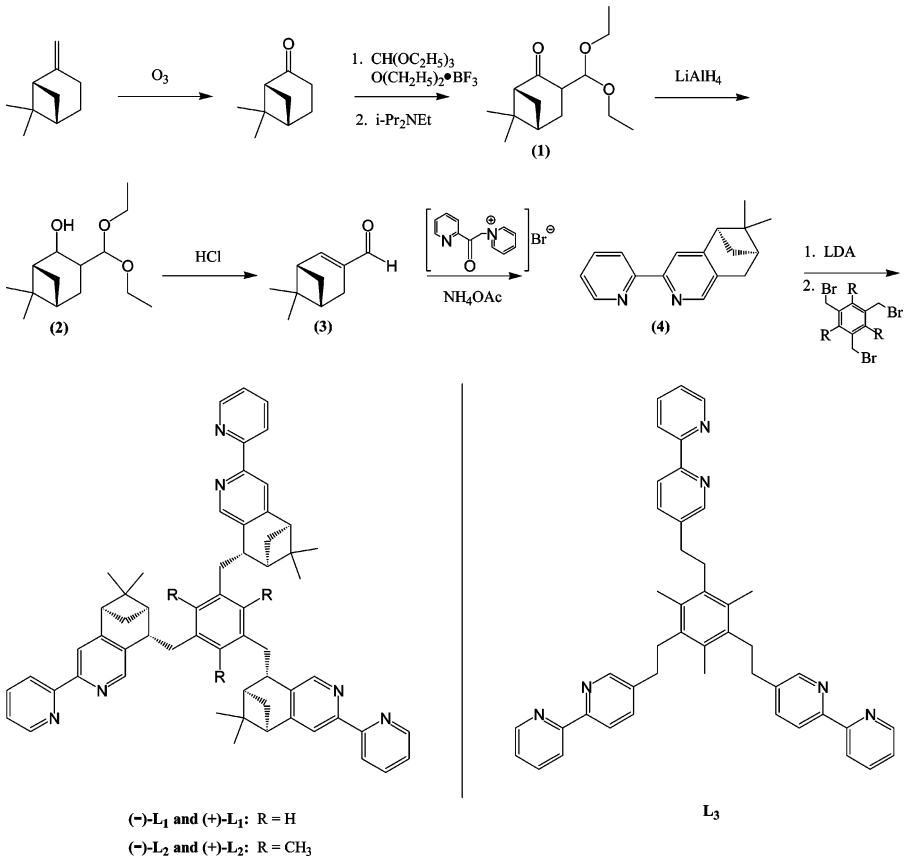

Figure 2. Synthetic pathway for the chiral, pbpy caged ligands. The path shown is that of **(−)-L$_1$** and **(−)-L$_2$**; ligands **(+)-L$_1$** and **(+)-L$_2$** used precursors possessing the inverse stereochemistry. An achiral bpy caged ligand, **L$_3$**, is also shown at right; upon complexation to a metal ion, the resulting compounds from this ligand form in a racemic mixture of Δ and Λ isomers.

of a mesityl-linking group used in place of the simple phenyl linker. It is important to note that the novel structure of the 4,5-pineno-2,2′-bipyridine moiety achieved through this synthetic pathway enables new strategies for tailoring these ligand systems to a variety of applications similar to those of its two cousins (Figure 1a,b). An achiral, hemicage bpy ligand (**L$_3$**) was also synthesized and is depicted in Figure 2 as well; upon coordination to a metal ion, this ligand leads to the formation of racemic complexes. The metal complexes of Ru(II) or Zn(II) were synthesized through complexation with $Ru(DMSO)_4Cl_2$ and $ZnCl_2$, respectively, and isolated as the PF_6^- salt.

Ruthenium Caged Complexes. 1. Luminescence and Absorption. Our initial studies of these caged bipyridyl complexes were focused on the use of a simple mesityl linker between three unmodified bipyridine units, similar to the complexes studied by Beeston and co-workers.[13,28] As in that previous work, our racemic ruthenium complex, [Ru(**L$_3$**)]$(PF_6)_2$, showed a large increase in excited-state lifetime and photoluminescent quantum yield over that of the uncaged [Ru(bpy)$_3$]$(PF_6)_2$ species (Table 1). This increase was attributed to the ligand sphere's higher rigidity which reduces the rate constant of vibrational, nonradiative decay (k_{nr}).

Along that line of reasoning, one would expect the hemicage pineno-2,2′-bipyridine species to exhibit an even greater enhancement of the quantum yield and lifetime owing to the presence of additional rigid substituents. However, what is observed is a large decrease in both quantities in comparison to the racemic cage, [Ru(**L$_3$**)]$(PF_6)_2$. In the case of the mesityl-capped diastereomers, Δ-[Ru(**(−)-L$_2$**)]$(PF_6)_2$ and Λ-[Ru(**(+)-L$_2$**)]$(PF_6)_2$, the efficiency and lifetime are still comparable to those of uncaged Ru(bpy)$_3$]$(PF_6)_2$ at 8.4% and 0.87 μs, respectively. For the phenyl-capped diastereomers Δ-[Ru(**(−)-L$_1$**)]$(PF_6)_2$ and Λ-[Ru(**(+)-L$_1$**)]$(PF_6)_2$, the efficiency and lifetime are drastically reduced to 1.0% and 0.12 μs. The cause of these reductions in relation to the racemic cage is not immediately clear. The most likely explanation is the presence of the additional hydrogen atoms associated with the pinene substituents; these atoms increase the overall vibrational freedom of the complex and can thus provide additional pathways for nonradiative decay and inhibit luminescence. Additionally, it is possible that the extra bulk of the pinene substituents can slightly distort the complex and causes a subtle deviation from the favored geometry, thus lowering the overall quantum efficiency.

Table 1. Photophysical Properties of Ru(II) Compounds

compound	absorbance maximum MLCT (nm)	emission maximum (nm)	Φ_{PL}	τ (μs)
[Ru(bpy)$_3$]$(PF_6)_2$	451	605	0.062	1.14
[Ru(**L$_3$**)]$(PF_6)_2$	454	595	0.237	3.28
Δ-[Ru(**(−)-L$_1$**)]$(PF_6)_2$	468	603	0.010	0.12
Δ-[Ru(**(−)-L$_2$**)]$(PF_6)_2$	468	603	0.084	0.87

(28) Beeston, R. F.; Larson, S. L.; Fitzgerald, M. C. *Inorg. Chem.* **1989**, *28*, 4187−4189.

(29) Frisch, M. J.; et al. *Gaussian 03*, revision C.02; Gaussian, Inc.: Wallingford, CT, 2004.

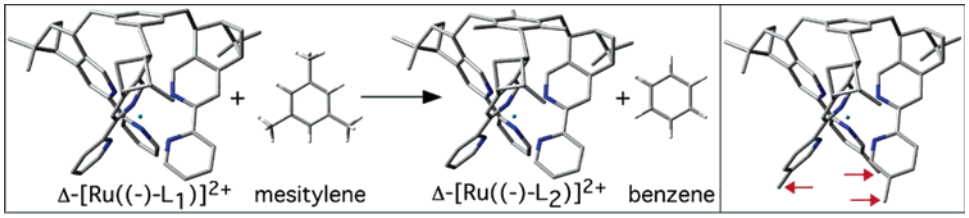

Figure 3. (Left) Isodesmic reaction of Δ-[Ru((−)-**L**$_1$)]$^{2+}$ with mesitylene to form Δ-[Ru((−)-**L**$_2$)]$^{2+}$ and benzene is shown. DFT calculations showed that the mesitylene-capped complex is more highly strained by 14.7 kcal/mol. (Right) Structural isomer of Δ-[Ru((−)-**L**$_2$)]$^{2+}$ used as a stand-in for Δ-[Ru((−)-**L**$_1$)]$^{2+}$ for purposes of ZPE comparison; red arrows indicate the location of the additional methyl groups. DFT calculations showed that the ZPE of the mesityl-capped complex was higher by 1.7 kcal/mol.

To investigate the higher luminescent performance of the mesityl-capped complexes over the phenyl-capped, density functional theory (DFT) calculations at the B3LYP/LANL2DZ level were carried out using Gaussian 03.[29] An isodesmic reaction was used to compare the amount of steric strain between the phenyl-capped Δ-[Ru((−)-**L**$_1$)]$^{2+}$ and the mesityl-capped Δ-[Ru((−)-**L**$_2$)]$^{2+}$ (Figure 3, left). As expected, the more crowded mesityl cap proved to be more strained by 14.7 kcal/mol. Additionally, to understand better the enhanced performance of the mesityl-capped complexes, the zero-point energies (ZPE) of the compounds were also calculated. To compare the energies for these two types of complexes by calculation, it is necessary that the specific compounds to be compared are isomeric. In this case, the phenyl-capped complex was converted into a structural isomer of the mesityl-capped variety through the addition of three methyl groups at the 5′ positions of the bipyridine rings, a location that causes minimal steric hindrance and thus should serve as an effective analogue (Figure 3, right). These calculations demonstrate that the ZPE of the mesityl-capped Ru complex is larger (1.7 kcal/mol) than that of the phenyl-capped isomer. The higher ZPE corresponds to increased rigidity of the compound, which should lower the rate of nonradiative decay within the complex and can thus help to explain the increase in quantum efficiency of the mesityl-capped compounds.

The absorption and emission spectra of the ruthenium complexes are displayed in Figure 4. The emission spectra of Ru(bpy)$_3$(PF$_6$)$_2$ and the pinenobipyridyl complexes are very similar with emission maxima at 605 and 603 nm, respectively. The absorption spectra of the complexes are also reasonably similar, with a notable exception occurring in the metal-to-ligand charge transfer (MLCT) region between 350 and 500 nm. The pinenobipyridyl complexes are all red-shifted to 468 nm from the 451-nm absorption observed for Ru(bpy)$_3^{2+}$, further suggesting a slight distortion of the ligand sphere.

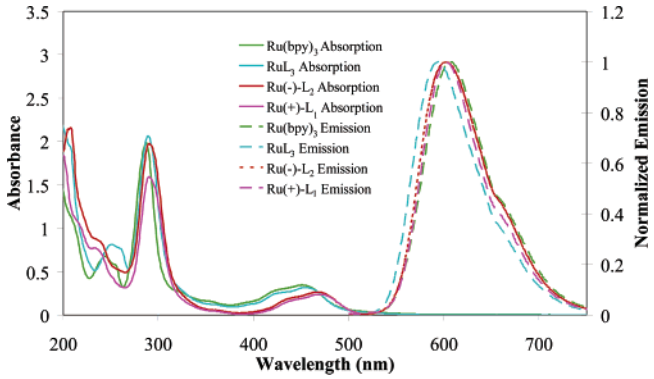

Figure 4. Combined absorption and uncorrected emission spectra of Ru(II) hemicage complexes.

2. Chiroptical Properties. CD spectra of the two mesityl-capped Ru(II) cages are shown in Figure 5. The complexes each show a Cotton effect at 282 and 299 nm, and the Δϵ values are of opposite sign for each enantiomer, clearly indicating that predetermination of the helicity at the metal center was successful.

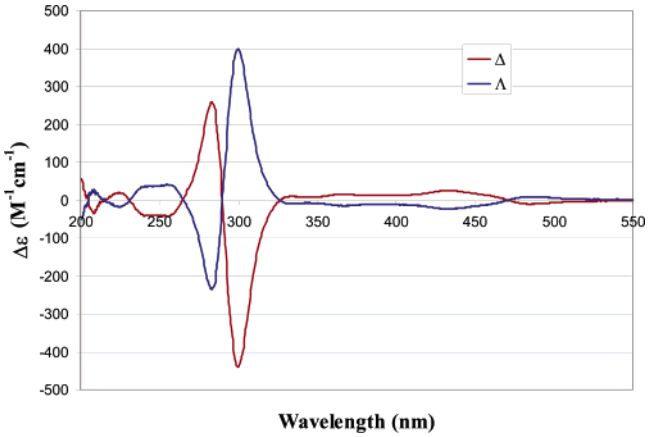

Figure 5. CD spectra of Δ-[Ru((−)-**L**$_2$)](PF$_6$)$_2$ (red) and Λ-[Ru((+)-**L**$_2$)](PF$_6$)$_2$ (blue). The samples were 25 μM in acetonitrile.

Figure 6 shows the CPL data for the phenyl-capped Ru(II) cages, Δ-[Ru((−)-**L**$_1$)](PF$_6$)$_2$ and Λ-[Ru((+)-**L**$_1$)](PF$_6$)$_2$. At 600 nm, the values of g_{em} are equal to $-7.3\ (\pm 0.6) \times 10^{-4}$ and $7.7\ (\pm 0.6) \times 10^{-4}$ for the Δ and Λ, respectively. These complexes show a slight decrease in g_{em} as wavelength increases, consistent with work by Gafni and Steinberg conducted on [Ru(bpy)$_3$]$^{2+}$ complexes.[30]

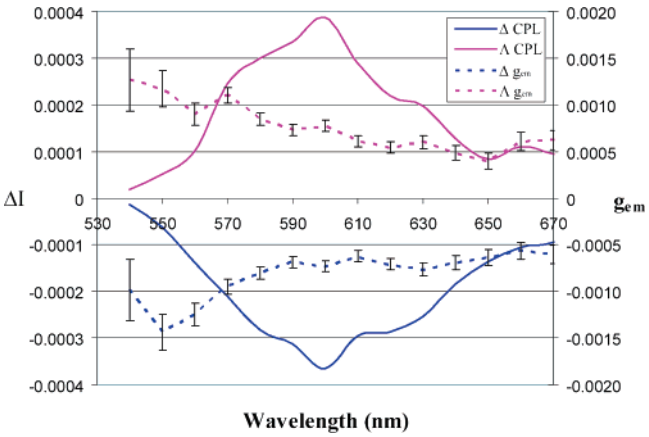

Figure 6. CPL spectra (solid lines) and emission dissymmetry values (dashed lines) of Δ-[Ru((−)-**L**$_1$)](PF$_6$)$_2$ (blue) and Λ-[Ru((+)-**L**$_1$)](PF$_6$)$_2$ (pink). Samples were 25 μM in acetonitrile and degassed prior to collection of their spectra (excited at $\lambda = 450$ nm).

The mesityl-capped Ru(II) cages, Δ-[Ru(**(−)-L$_2$**)](PF$_6$)$_2$ and Λ-[Ru(**(+)-L$_2$**)](PF$_6$)$_2$, also show similar spectra, with values of g_{em} equaling −5.3 (±0.2) × 10^{-4} and 5.5 (±0.3) × 10^{-4} for the Δ and Λ isomers, respectively, as seen in Figure 7. Although the signal varies, it is important to note that opposite CPL signals were recorded for each set of diastereomers, indicating that the CPL is caused by the arrangement of the ligands around the metal center. In addition, the g_{em} values for our Ru(II) cages are consistent with those of previously reported complexes that were separated through cocrystallization.[27,31]

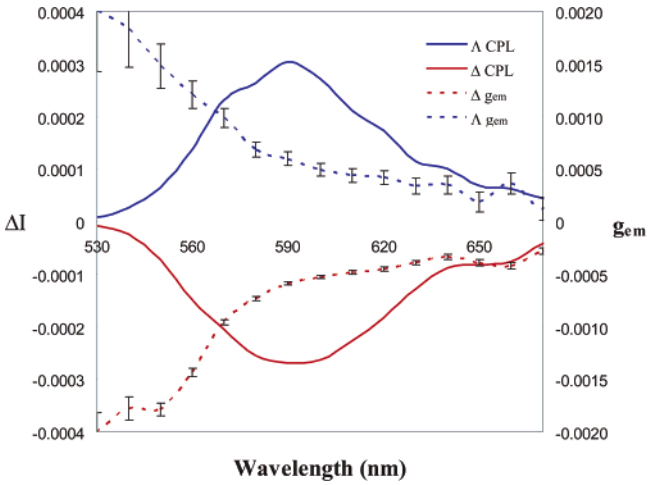

Figure 7. CPL spectra (solid lines) and emission dissymmetry values (dashed lines) of Δ-[Ru(**(−)-L$_2$**)](PF$_6$)$_2$ (red) and Λ-[Ru(**(+)-L$_2$**)](PF$_6$)$_2$ (blue). Samples were 25 μM in acetonitrile and degassed prior to collection of their spectra (excited at λ = 450 nm).

Zinc Caged Complexes. 1. Luminescence and Absorption. As was done for the Ru(II) case, a racemic caged bipyridyl complex from Zn(II), [Zn(**L$_3$**)](PF$_6$)$_2$, was synthesized and its photophysical properties were compared to those of the uncaged complex. For the parent [Zn(bpy)$_3$](PF$_6$)$_2$ complex, an intense emission was observed in the UV region at 326 nm (Figure 8).

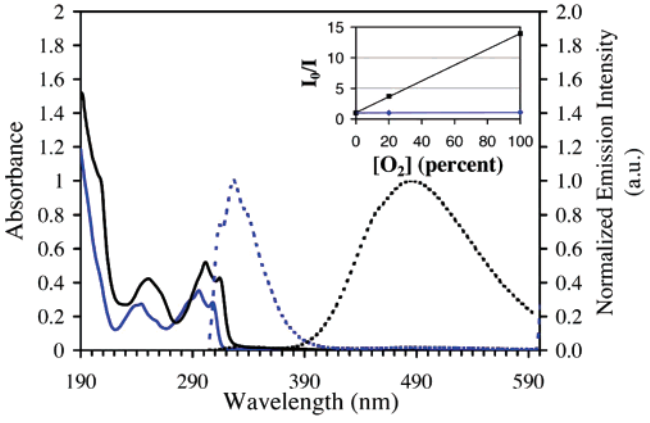

Figure 8. Combined absorption (solid lines) and emission (dashed lines) of [Zn(bpy)$_3$](PF$_6$)$_2$ (blue) and racemic [Zn(L$_3$)](PF$_6$)$_2$ (black). A Stern−Volmer plot of the effect of diatomic oxygen quenching is depicted in the inset. No quenching was observed for the fluorescent [Zn(bpy)$_3$](PF$_6$)$_2$, whereas the phosphorescence of [Zn(L$_3$)](PF$_6$)$_2$ was strongly quenched.

This emission appears to be fluorescent based on the short-lived (<10 ns) excited-state lifetime and the resistance to oxygen quenching (Figure 8, inset). The addition of the mesityl cap to form [Zn(**L$_3$**)](PF$_6$)$_2$ drastically affected the emission spectrum of the complex. The previously strong fluorescence in the UV region becomes almost negligible, while a new, broad peak centered around 485 nm is observed instead. This emission proved to be phosphorescence, based on the relatively long-lived excited-state lifetime (τ = 0.089 μs) and the observance of quenching by oxygen, as shown by the linear increase of I_0/I as the concentration of O_2 was increased. The quenching constant (k_q) was calculated to be 1.5 × 10^9 M^{-1} s^{-1} through the Stern−Volmer equation (eq 3), where [Q] is the concentration of the quencher, O_2:

$$I_0/I = 1 + k_q\tau_o[Q] \qquad (3)$$

Because Zn(II) complexes are d^{10}, it can be assumed that this transition does not involve the metal orbitals and is of a triplet ligand-centered (^{3}LC) nature. The shift in the energy maximum from the fluorescent tris-bipyridine complex (λ_{max} = 326 nm) to the phosphorescent cage complex (λ_{max} = 485 nm) amounts to 1.24 eV, comparable to singlet−triplet energy gap values given by Turro for aromatic molecules possessing π structure similar to that of bipyridine.[32] Photophysical measurements for the Zn(II) complexes are summarized in Table 2.

Table 2. Photophysical Properties of Zn(II) Compounds

compound	absorbance maximum (nm)	emission maximum (nm)	Φ_{PL}	τ (μs)
[Zn(bpy)$_3$](PF$_6$)$_2$	295	326	0.571	<0.010
[Zn(**L$_3$**)](PF$_6$)$_2$	301	485	0.069	0.089
Δ-[Zn(**(−)-L$_2$**)](PF$_6$)$_2$	302	470	0.108	0.074

A possible rationalization for the nearly complete switch from singlet emission to triplet emission is the addition of the mesityl cap itself. Hexa-alkyl substituted benzenes have previously been shown to possess a triplet excited state similar in energy[33] to that of 2,2′-bipyridine.[34,35] Therefore, the presence of this additional triplet state provided to the complex by the mesityl cap offers another possible radiative pathway through which the compound can return to the ground state. Assuming good vibrational overlap between the excited singlet state and the various triplet states, intersystem crossing between these levels could be strongly encouraged and thus cause the switch to phosphorescent emission. Additionally, the greater rigidity of the caged ligand sphere could prevent significant rearrangements of the excited states and assist in providing good vibrational overlap and thereby increase the rate constant for intersystem crossing, k_{isc}. This enhancement of phosphorescence could be of use to the field of organic light emitting devices (OLEDs), seeing as current emphasis in OLED design has been on the use of molecules emitting from the triplet state. Very high efficiency devices are thought to only be possible through the use of phosphorescent emission, which should theoretically

(30) Gafni, A.; Steinberg, I. Z. *Isr. J. Chem.* **1977**, *15*, 102−105.
(31) Blok, P. M. L.; Cartwright, P. S.; Dekkers, H. P. J. M.; Gillard, R. D. *J. Chem. Soc., Chem. Commun.* **1987**, 1232−1233.
(32) Turro, N. J. *Modern Molecular Photochemistry*; University Science Books: Mill Valley, CA, 1991.
(33) Shizuka, H.; Ueki, Y.; Iizuka, T.; Kanamaru, N. *J. Phys. Chem.* **1982**, *86*, 3327−3333.
(34) Vinodgopal, K.; Leenstra, W. R. *J. Phys. Chem.* **1985**, *89*, 3824−3828.
(35) Ikeyama, T.; Okabe, N.; Azumi, T. *J. Phys. Chem. A* **2001**, *105*, 7144−7150.

allow all injected electron−hole pairs to become triplet excitons capable of light emission.[36]

The combined emission and absorption spectra of the mesityl-capped Zn(II) pinenobipyridine cages are shown in Figure 9. The emission is a single, broad peak of blue-white luminescence centered around 470 nm. As with $[Zn(\mathbf{L}_3)](PF_6)_2$, lifetime measurements (Table 2) and oxygen quenching studies of the complexes indicate that the luminescence is phosphorescent in nature. The quenching constant was $1.3 \times 10^9\ M^{-1}\ s^{-1}$, a value smaller than that observed for the racemic compound; this result can be rationalized by the greater steric bulk provided by the pinene units which could partially shield the complex from the oxygen quencher.

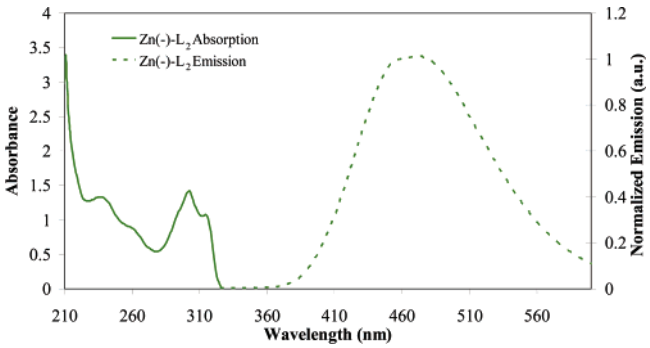

Figure 9. Combined absorption and emission spectra of Δ-[Zn(**(−)-L$_2$**)]-$(PF_6)_2$.

2. Chiroptical Properties. The CD spectra for the Zn(II) mesityl-capped chiral cages are shown in Figure 10. A Cotton effect of equal and opposite relationship was observed at 316 nm for the diastereomers. It is noteworthy that the complexes remained stable over the course of months with no observable racemization.

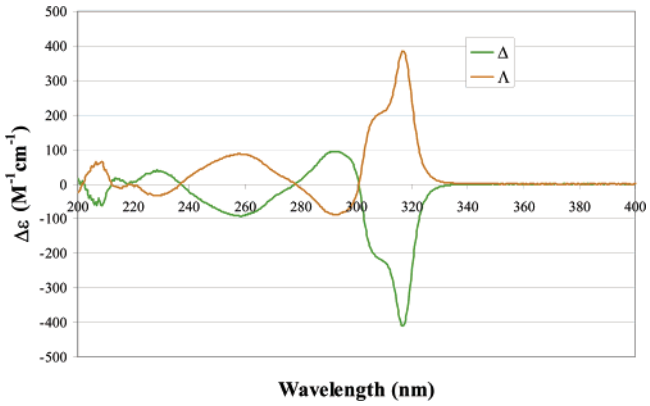

Figure 10. CD spectra of Δ-[Zn(**(−)-L$_2$**)]$(PF_6)_2$ (green) and Λ-[Zn(**(+)-L$_2$**)]$(PF_6)_2$ (orange). The samples were 25 μM in acetonitrile.

Figure 11 displays the CPL data for the Zn(II) mesityl-capped cage complexes. For each complex, the CPL is essentially constant from 430 to 560 nm, indicating that there is only one transition in this region. This transition has a g_{em} of $-2.4\ (\pm 0.1) \times 10^{-3}$ and $2.4\ (\pm 0.1) \times 10^{-3}$ at 460 nm for the Δ and Λ isomers, respectively; this corresponds to light that is 0.12% circularly polarized. To our knowledge, these are the first reported CD and CPL spectra for luminescent Zn(II) complexes with predetermined configuration at the metal center.

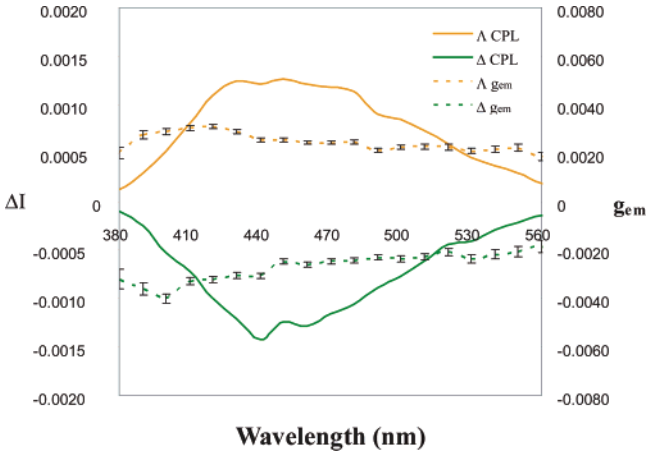

Figure 11. CPL spectra (solid lines) and emission dissymmetry values (dashed lines) of Δ-[Zn(**(−)-L$_2$**)]$(PF_6)_2$ (green) and Λ-[Zn(**(+)-L$_2$**)]$(PF_6)_2$ (orange). Samples were 25 μM in acetonitrile and degassed prior to collection of their spectra (excited at $\lambda = 315$ nm).

Conclusions

We have synthesized both enantiomers of a new, pinene-substituted 2,2′-bipyridine ligand with broad potential applications in the fields of asymmetric catalysis and the stereoselective synthesis of metal complexes. The ligand can readily be substituted with a linking spacer to form a hemicaged species capable of forming chiral metal complexes of Ru(II) and Zn(II) with complete selectivity, as was shown through both CD and CPL measurements. Additionally, the Zn(II) complexes were shown to display a heretofore unprecedented switching from fluorescent to phosphorescent emission between the uncaged $Zn(bpy)_3^{2+}$ and the hemicaged species. Such an enhancement of phosphorescent emission could lead to future discoveries of efficient triplet emitters for use in ionic OLED applications.

Acknowledgment. This work was supported by the National Science Foundation (Career Award No. CHE-0449755) and a Camille and Henry Dreyfus Foundation New Faculty Award. F.J.C. acknowledges support by a National Science Foundation Graduate Research Fellowship.

Supporting Information Available: Complete citation for ref 29 as well as NMR and mass spectrometry data for key metal compounds. This material is available free of charge via the Internet at http://pubs.acs.org.

JA067016V

(36) Forrest, S. R. *Org. Electron.* **2003**, *4*, 45−48.